

Influence of Surface Nanocrystallization on Aluminizing Behavior of AZ91D Magnesium Alloy

Zhang Conghui^{1,2}, Song Guodong¹, Wang Jing¹, Zhao Xu¹

¹Xi'an University of Architecture and Technology, Xi'an 710055, China; ²Shaanxi Metallurgical Engineering Technology Research Center, Xi'an 710055, China

Abstract: Surface aluminizing for magnesium alloy is an effective method to improve corrosion resistance. This research introduced surface nanocrystallization as the pre-process of aluminizing. AZ91D magnesium alloy was processed by high energy shot peening (HESP) to achieve surface nanocrystallization, and then vacuum solid state aluminum diffusion was performed to obtain aluminized layer. The morphology of the aluminized layer was observed by transmission electron microscopy (TEM) and scanning electron microscopy (SEM). The results show that the surface of the nanocrystalline with grain size of 100 nm is obtained after HESP of AZ91D magnesium alloy. The depth of the HESPed aluminized layer is thicker than that of the aluminized layer without HESP. After 440 °C/12 h diffusion, the depth of aluminized layer increases to 70 μm. The corrosion resistance of AZ91D magnesium alloys were characterized by electrochemical method. It is shown that the aluminized layer obviously lowers the corrosion rate of AZ91D magnesium alloy. Therefore, high energy shot peening (HESP) is beneficial to surface aluminizing and can improve the corrosion resistance of magnesium alloy.

Key words: high-energy shot peening; surface nanostallization; aluminum diffusion; corrosion resistanc

The magnesium alloy has various advantages: high thermal and electric conductivity, high specific modulus and specific strength, good shield effectiveness to electromagnetic disturbance, and so on^[1-3]. Therefore, it is extensively applied in a variety of industrial domains, such as communication, automobiles, and aerospace^[4-7]. However the standard electrode potential of magnesium element is extremely low, being only -2.37 V, besides, it cannot automatically generate self-protective film on magnesium surface, leading to its low corrosion-resistance in many media, thereby largely restraining practical application of magnesium alloy. The corrosion resistance of magnesium alloy can usually be improved by two aspects: limiting the content of impurity elements such as iron, nickel, copper, cobalt, etc. to reduce severe galvanic corrosion, and the surface treatment of magnesium alloy to enhance the corrosion-resistance of surface film^[8-10]. As a widely applied surface treatment,

thermal diffusion is a high-temperature processing, the surface layer achieves metallurgical bonding between substrate metal and diffusion metal^[11,12]. With binding force is better than that of other surface treatment modes for magnesium alloy, and it does not influence the heat conduction and electromagnetic shielding effect of magnesium alloy. The aluminizing for magnesium alloy introduces passivating metallic aluminum into the surface layer and changes the components and structure of alloy surface, thereby improving the corrosion-resistance of magnesium alloy^[13-15]. Wang et al^[16] employed permeation method of solid state metal powder and achieved alloy diffusion layer on magnesium alloy successfully. High energy shot peening (HESP) can introduce nanocrystallized surface layer and residual stress by grains refinement. The presence of nanolayer and residual stress could influence the channel for atomic diffusion, thus it is expected to improve aluminum diffusion behavior during aluminizing. The paper

Received date: February 25, 2019

Foundation item: Key Projects of Science and Technology Research of the Ministry of Education (211178); Yulin Municipal Science and Technology Bureau Project (2014cxy-05)

Corresponding author: Zhang Conghui, Ph. D., Professor, School of Metallurgical Engineering, Xi'an University of Architecture and Technology, Xi'an 710055, P. R. China, Tel: 0086-29-82202547, E-mail: jiandazhang2010@hotmail.com

Copyright © 2020, Northwest Institute for Nonferrous Metal Research. Published by Science Press. All rights reserved.

discussed the aluminum diffusion behavior in magnesium alloy before and after nanocrystallization, and researched its thickness of diffusion layer and corrosion behavior to uncover the influence of surface nanocrystallization on aluminum diffusion behavior.

1 Experiment

The samples for surface nanocrystallization were selected from the raw materials—commercial AZ91D magnesium alloy cast ingot, they were processed into plate samples with size of 100 mm×100 mm×10 mm via wire electrical discharge machining (WEDM). The samples were subjected to HESP with shot peening pressure of 0.2 MPa for 30 min. After HESP, the plate samples were cut into 10 mm×10 mm blocks. The samples were rinsed by immersion into acetone and alcohol with ultrasonic cleaning for 10 min, and then washed them with ionized water, and dried, and the dried material was to be used for aluminum power permeation. The samples were placed in aluminizing powder which was paved with the thickness of 2 cm on the bottom of iron crucible. After aluminum powder covered and compacted the samples, the aluminum foil was used for enveloping and sealing the samples. The crucible was moved into aluminizing pot, which was then covered and placed into electric heater (temperature was controllable). For the convenience of detection and analysis, its surface should be cleaned firstly. Full argon, after temperature achieved set standard, the electricity was disconnected to cool the pot naturally before the samples were taken out. At 440 °C, 8 h and 12 h of diffusion aluminizing were carried out, respectively.

The JEM-2100 transmission electron microscope was used to observe the surface characteristics of nanocrystallized surface. The samples were prepared via ion milling: firstly cut about 0.5 mm thick flakes from the surface, reserving the nanocrystallized surface, and grinding it on metallographic abrasive paper to 50 μm, then punching and pre-thinning it, and using ion mill for final thinning. The diffusion layer's morphology on section of samples was observed using SEM (HITACHI S-2400), and the thickness of diffusion layer was determined. The energy disperse spectroscopy (EDS) was adopted to analyze the components and elements distribution on cross section of diffusion layer. The X-ray diffractometer was used to make phase analysis on surface of diffusion layer to define phase composition of surface.

The corrosion behaviors of sample were tested by potentialdynamic polarization and electrochemical impedance. The electrochemical test was carried out used PARSTAT4000 electrochemical workstation, and conducted in 3.5 wt% NaCl solution with standard three-electrode system. The samples were embedded in epoxy resin, with 1 cm² exposed on the surface area serve as work electrode, while the reference and counter electrode were saturated calomel and platinum material. The polarized scanning of electrokinetic potential was conducted at a rate of 1 mV/s, and the impedance data

was fitted via Zsimp Win 3.2 software. The impedance frequency and alternating current (AC) amplitude value was set as 10 mHz~100 kHz and 10 mV, respectively.

2 Results and Discussion

2.1 Morphology after high energy shot peening

Fig.1 is the TEM images of AZ91D magnesium alloy, the bright field image and dark field image of the original sample are shown in Fig.1a and 1b, the bright field image and dark field image on the surface of samples after HESP are shown in Fig.1c and 1d. Dislocation lines appear in the grains of the original sample. It is observed that after HESP, the grain size of AZ91D magnesium alloy surface are significantly refined, and it shows that the size is refined to 100 nm. The grain size of raw material AZ91D magnesium alloy in cast state is in micron order. The grains were broken continuously under the action of HESP to generate substantive nanometer grains. The results show that the treatment for 30 min under the pressure of 0.2 MPa is optimal and can obtain the finest nanometer grains.

2.2 Morphology and EDS, XRD analysis of the diffusion layer

Fig.2 is the SEM images of cross section after aluminum diffusion for AZ91D magnesium alloy. Fig.2a, 2b are graphs for diffusion aluminized, Fig.2c, 2d are images for diffusion aluminized after HESP, wherein the permeation time in Fig.2a, 2c is 8 h, and in Fig.2b, 2d is 12 h. As seen in Fig.2, it shows that all the surfaces of samples produce permeable layers with different thickness. As diffusion time increase, the aluminized coating becomes thicker and thicker. In the same diffusion conditions, the diffusion layer of samples with HESP is significantly thicker than that of the samples without HESP. And after HESP, the thickness of the aluminized layer is the largest at 12 h, being 70 μm. It indicates that HESP can enhance permeation velocity of aluminum element in the magnesium alloy, thus within the same diffusion time, the samples after HESP treatment have thicker aluminized coating. The HESP can increase the roughness of sample surface, and introduce substantive nanometer grain boundaries, which introduced diffusion channels for aluminum element, thereby raising the diffusion velocity.

To further determine the thickness and components distribution of permeation layer, the EDS analysis was carried out on cross section of diffusion layer. Fig.3a is the SEM image of diffusion layer and neighboring substrate after diffusion treatment at 440 °C for 12 h after HESP. Fig.3b shows the distribution of Mg element and Al element on the straight line in Fig.3a. It is observed from Fig.3a that the aluminized coating and substrate are perfectly bonded, being very firm. In addition, the microstructure of aluminized coating is uniform and compact with substrate structure, it is found that compared with the substrate, the content of aluminum in diffusion layer is higher, aluminum content increase from the substrate to the surface, while the magnesium content in substrate is significantly higher than in diffusion layer. It shows

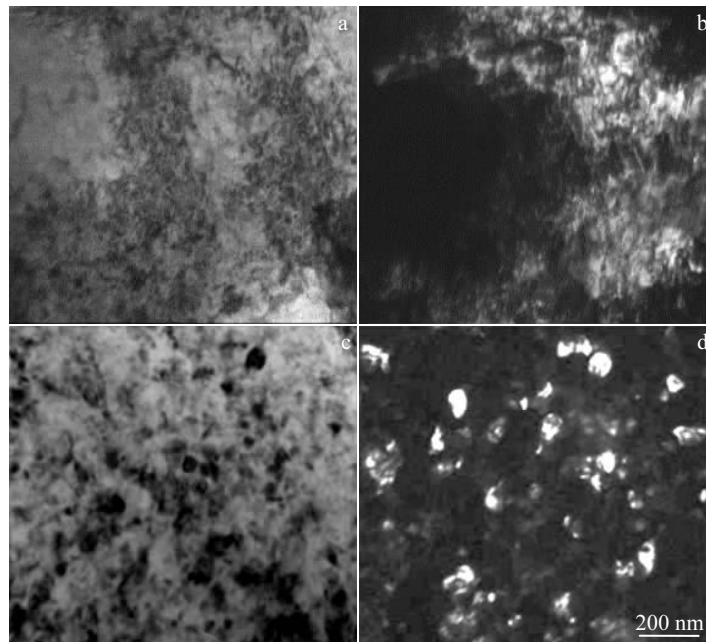


Fig.1 TEM bright field images (a, c) and dark field images (b, d) on the surface of AZ91D magnesium alloy: (a, b) original sample and (c, d) after HESP

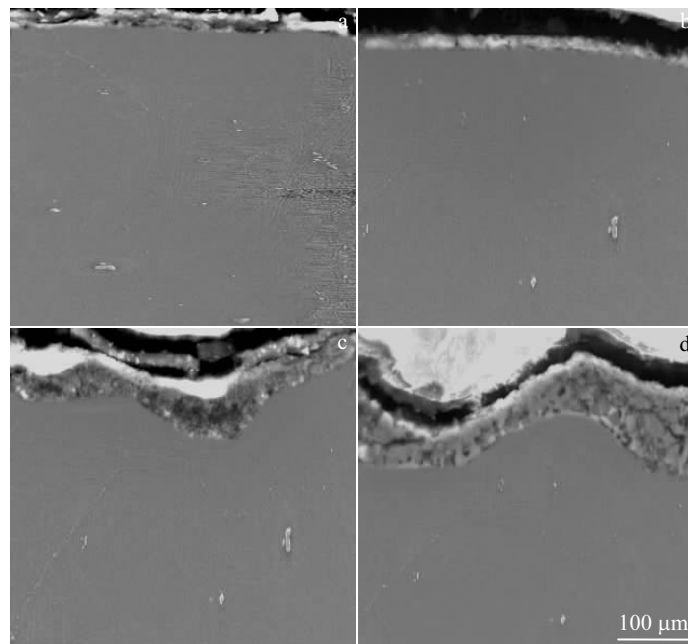


Fig.2 SEM images of cross-section of aluminizing samples: (a) 440 °C/8 h, (b) 440 °C/12 h, (c) HESP+440 °C/8 h, and (d) HESP+440 °C/12 h

that the diffusion layer contains two elements of aluminum and magnesium, and magnesium is the majority. During the whole permeation process, the two elements take on interpenetration, and the bonding between diffusion layer and substrate is good.

To further determine the phase composition of diffusion layer, the X-ray diffractometer is used to test the surface of original sample and treated sample. As shown in Fig.4, pattern a is the pattern of original sample, pattern b is the pattern of sample permeated at 440 °C for 12 h after HESP. It is

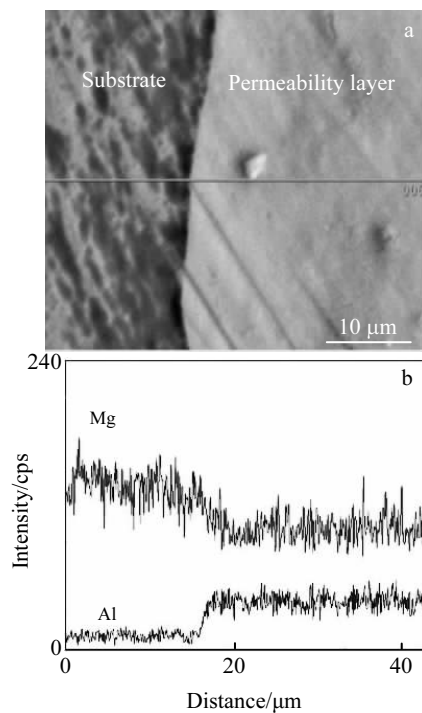


Fig.3 Cross-sectional SEM image (a) and EDS line scanning (b) of AZ91D magnesium alloy for aluminizing HESPed sample

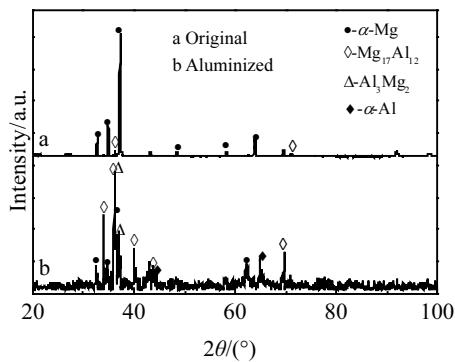


Fig.4 XRD patterns of AZ91D magnesium alloy before and after aluminizing

observed from the figure that the original sample is composed of two phases of α -Mg and $Mg_{17}Al_{12}$, with a few content of the second phase. After aluminizing, the peak position and peak value for $Mg_{17}Al_{12}$ phase increase obviously and the peak of Al_3Mg_2 and α -Al phase appears. According to the peak position and peak value, it can be seen that the diffusion layer is mainly composed of two components, i.e. $Mg_{17}Al_{12}$ and Al_3Mg_2 . Related research showed that the outermost layer of diffusion layer is single-phase Al_3Mg_2 layer, on which is bonded with some α -Al grains, the sub-surface layer is single-phase $Mg_{17}Al_{12}$ layer, and inner layer is composed of two phases of α -Mg and $Mg_{17}Al_{12}$.

2.3 Microhardness analysis

Fig.5 is the distribution curves of surface microhardness of aluminizing alloy along the direction of depth of diffusion layer. It shows that compared with the substrate, the diffusion layer has higher microhardness. The hardness of AZ91D magnesium alloy substrate is 600 MPa, while the diffusion coating is 1800 MPa, 3 times higher than the substrate. The reason responsible for such difference is that substantive intermetallics Al_3Mg_2 and $Mg_{17}Al_{12}$ disperse into the diffusion layer, while these compounds are all strengthening phase with high hardness.

2.4 Research on electrochemical properties

To find out the influence of surface treatment on corrosion resistance of alloy, the potentiodynamic polarization and impedance spectrum of original samples and aluminized samples were researched. Fig.6 shows the potentiodynamic polarization curves of AZ91D alloy before and after aluminizing. It is observed from the figure that the polarization behavior of alloy does not change significantly, and the polarization curve is composed of hydrogen evolution on cathode and anodic solution, the anodic curve after aluminizing has no significant passivating. After HESP and aluminizing, all of the self-corrosion potential move towards positive potential, indicating HESP and aluminizing can inhibit anodic reaction to a certain extent. Table 1 shows self corrosion potential and current density corresponding to the samples in Fig.6. The corrosion current data in the Table shows that the current density of original sample is $243.675 \mu A/cm^2$, while the current density of sample after HESP increases to $544.050 \mu A/cm^2$, while aluminizing increases the corrosion resistance of original and HESP alloys, the corrosion current density of alloy subjected to permeated at $440^\circ C$ for 12 h after HESP is the smallest, being $41.860 \mu A/cm^2$. As HESP increases the roughness of alloy surface, and produces a stress layer on alloy surface, the corrosion current density of HESP alloy increases, while aluminizing after HESP increases the thickness of diffusion layer and the aluminum content, so the current density after aluminizing reduces remarkably, and corrosion resistance is improved. With the increase of permeation time, the

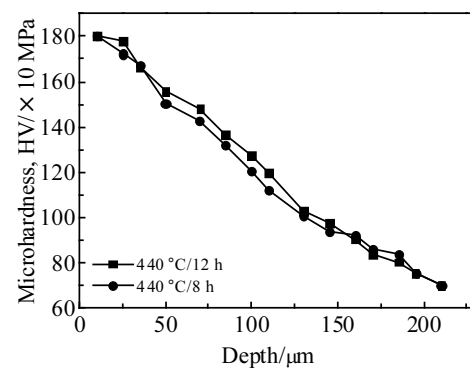


Fig.5 Distribution of microhardness of the samples after aluminum diffusion along the depth of aluminizing

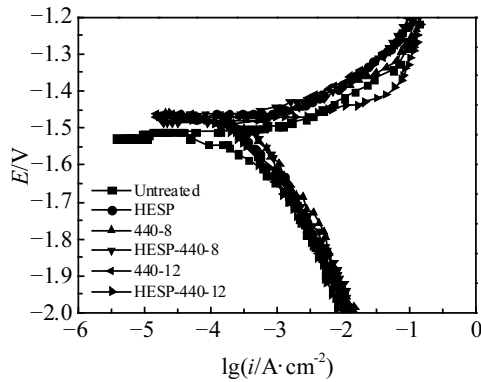


Fig.6 Electrochemical polarization curves of AZ91D magnesium alloy before and after surface diffusion

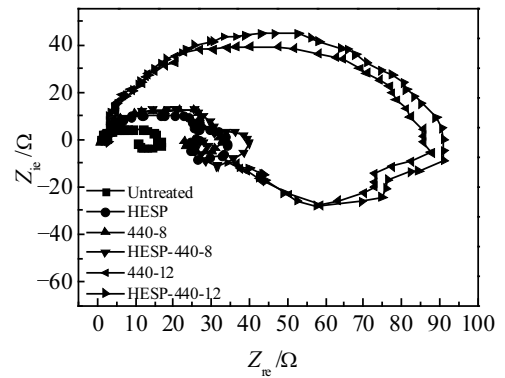


Fig.7 EIS of AZ91D magnesium alloy in 3.5 wt% NaCl solution before and after surface diffusion

Table 1 Corrosion potential and corrosion current density of AZ91D magnesium alloy

Treatment process	$E_{corr}^{[a]}/mV$	$i_{corr}^{[b]}/\mu A \cdot cm^{-2}$
Untreated	-1.506	243.675
HESP	-1.512	544.050
440-8	-1.481	243.675
HESP-440-8	-1.451	238.100
440-12	-1.476	92.870
HESP-440-12	-1.484	41.860

[a] self corrosion potential; [b] self corrosion current density

diffusion layer's thickness increases and current density declines. Therefore, the alloy subjected to permeation at 440 °C for 12 h after HESP has the optimal corrosion-resistance.

Fig.7 shows the AC impedance spectra of original sample and aluminized sample of AZ91D magnesium alloy. It can be seen that the impedance curves of the samples aluminizing and aluminizing after HESP are in substantial agreement, and composed of capacitance arc in high frequency region, capacitance arc in intermediate frequency region and inductive reactance arc in low-frequency region. This indicates that HESP and aluminizing do not change the corrosion mechanism of alloy, and surface films have similar basic features. After aluminizing, the impedance increases, the longer the aluminizing time is, the more significant the increase of impedance is. After HESP, the impedance of aluminized alloy is generally higher than that of the alloy directly aluminized without HESP. As the radius of impedance arc represents the alloy's resistance to abrasion^[17,18], the alloy subjected to permeation at 440 °C for 12 h after HESP has the highest impedance performance and the best corrosion resistance. The appearance of inductive reactance arc in alloy is because the alloy surface adsorbed corrosion products such as Mg(OH)₂ during the process of corrosion, which interacts with solution, leading to relaxation, thereby generating inductive reactance arc^[19]. The reason for appearance of capacitance arc in medium high frequency region

of curve is mainly ascribed to the charge after corrosion reaction occurs to magnesium alloy and the discharge phenomenon of electrical double-layer capacitor, while the reason for inductive capacitance arc in intermediate frequency region is mainly due to the intermediates produced after magnesium eroded, and the generation of inductive reactance is related to erosion and dissolution reaction of magnesium^[20,21].

The equivalent fitting was conducted for the curve in Fig.7 using equivalent circuit diagram as shown in Fig.8. The data corresponding to equivalent circuit obtained by fitting is shown in Table 2. Wherein, R_s represents solution resistance, R_t represents charge-transfer resistance of metal surface between electrolyte solutions, the larger the value is, the stronger the corrosion-resistance is. The closer to 1 of the n value, the more uniform and compact the surface of measured electrode is, the lower the possibility of pitting is. Table 2 shows that the resistance value of alloy subjected to permeation at 440 °C for 12 h after HESP is the biggest, being 207.300 Ω/cm².

The electrochemical test shows that thermal diffusion and aluminizing after HESP improves corrosion-resistance of AZ91D magnesium alloy in 3.5 wt% NaCl solution. At the normal temperature or in the humid environment, electrochemical reaction would occur between the magnesium and intermetallic when they contact vapor, wherein, magnesium metal dissolves on anode, and hydrogen evolves on cathode.

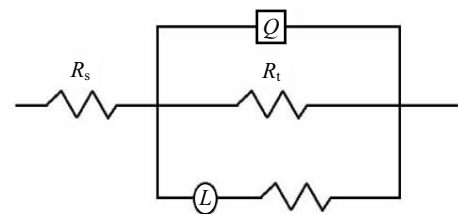


Fig.8 Equivalent circuit of AZ91D electrochemical impedance spectroscopy in NaCl solution

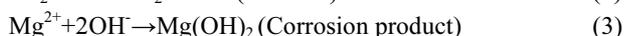
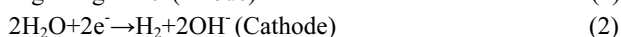
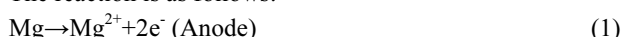
Table 2 Fitting parameters of equivalent circuit component

Treatment process	$R_s^{[a]}/\Omega \cdot \text{cm}^2$	$R_t^{[b]}/\Omega \cdot \text{cm}^2$	n
Untreated	9.824	79.110	0.894
HESP	4.774	77.200	0.880
440-8	1.987	109.300	0.897
HESP-440-8	8.436	144.200	0.890
440-12	5.619	164.300	0.860
HESP-440-12	5.784	207.300	0.850

^[a] solution resistance; ^[b] charge-transfer resistance

The dissolved magnesium ions and hydroxyls bond to generate magnesium hydroxide.

The reaction is as follows:



Thus, when the magnesium alloy contacts vapor, a layer of $\text{Mg}(\text{OH})_2$ corrosion products is formed on the surface of magnesium alloy substrate, while the generated $\text{Mg}(\text{OH})_2$ had low compactness with porous and loose surface, which could not well protect the magnesium alloy substrate. After aluminizing, it forms $\text{Mg}_{17}\text{Al}_{12}$ and Al_3Mg_2 compounds which are distributed like network on the surface of magnesium alloy. These network-like compounds could effectively protect magnesium alloy substrate, thereby improving the corrosion-resistance of substrate. Compared with magnesium substrate, the $\text{Mg}_{17}\text{Al}_{12}$ has relatively higher corrosion potential, and its corrosion current density in solution is lower, while the network-like distribution of $\text{Mg}_{17}\text{Al}_{12}$ can hinder contact of magnesium alloy substrate with solution. Research shows that presence of $\text{Mg}_{17}\text{Al}_{12}$ can highly postpone and prevent the action between solution and substrate and improve the corrosion-resistance of magnesium alloy in Cl⁻ environment^[22,23]. While the corrosion potential of Al_3Mg_2 compound is also higher than that of α -Mg, thus the presence of $\text{Mg}_{17}\text{Al}_{12}$ and Al_3Mg_2 can increase the resistance of magnesium alloy in chloride ion environment and improve corrosion-resistance of magnesium alloy.

3 Conclusions

1) After HESP, the surface of AZ91D magnesium alloy is nanocrystallized, and the grain size on surface layer is refined from micron order to nanometer order. The treatment for 30 min under pressure of 0.2 MPa is the optimal process, which can refine the grain size to 100 nm.

2) After HESP, the substantive nanometer grain boundaries on alloy surface provides better channels for diffusion of aluminum element during permeation, the thickness of diffusion layer is bigger than that of the original samples. The best aluminizing process is preserving heat for 12 h at 440 °C after HESP, and the thickness of diffusion layer is up to 70 μm .

3) After HESP, the alloy surface grain boundary defects and residual stress are introduced, the self corrosion current

density increases, and corrosion resistance declines. After aluminizing, the corrosion resistance of magnesium alloy is improved by the introduction of aluminized layer. The corrosion current density of magnesium alloy subjected to aluminum diffusion for 12 h at 440 °C after HESP is the smallest, being 41.860 $\mu\text{A}/\text{cm}^2$.

References

- Shi Xiuling. *Dissertation for Master*[D]. Chongqing: Chongqing University, 2010 (in Chinese)
- Sun Dexin, Sun Daqian, Li Jinbao et al. *Materials Review*[J], 2006, 20(8): 122 (in Chinese)
- Li Jiehua, Jie Wanqi, Yang Guangyu. *Rare Metal Materials and Engineering*[J], 2010, 39(1): 101 (in Chinese)
- Lin Zhixun. *Dissertation for Master*[D]. Shanghai: Shanghai Jiaotong University, 2008 (in Chinese)
- Guo Xingwu, Guo Jiacheng, Zhang Zhicheng et al. *Surface Technology*[J], 2017, 46(3): 53 (in Chinese)
- Xu Jianhui, Zhang Xuequn, Long Wenyuan. *Materials Science and Preparation Technology*[M]. Beijing: Science and Technology Press of China, 2001: 421 (in Chinese)
- Kang Hongyue, Chen Shanhua, Ma Yongping et al. *Metal World*[J], 2008(1): 61 (in Chinese)
- Zhu Liqun, Li Weiping, Lv Sainan. *Materials Science & Technology*[J], 2007, 15(2): 158 (in Chinese)
- Amy L Rudd, Camel B Breslin, Florian Mansfeld. *Corrosion Science*[J], 2000, 42: 275
- Yu Gang, Liu Yuelong, Li Ying et al. *The Chinese Journal of Nonferrous Metals*[J], 2002, 12: 1087 (in Chinese)
- Sun Xitai. *Material Surface Strengthening Technology*[M]. Beijing: Chemical Industry Press, 2005 (in Chinese)
- Kong Dezhun. *Principle of Chemical Heat Treatment*[M]. Beijing: Aviation industry press, 1992 (in Chinese)
- Sun An, Sui Xiaoming, Li Haitao et al. *Materials and Design*[J], 2015, 67: 280
- Chang H W, Zhang M X, Atrens A et al. *Journal of Alloys and Compounds*[J], 2014, 587: 527
- Hirmke J, Zhang M X, StJohn D H. *Surface and Coatings Technology*[J], 2011, 206: 425
- Wang Xiaodong, Li Yuandong, Chen Tijun et al. *Surface Technology*[J], 2011, 5: 41 (in Chinese)
- Yang Mingbo, Pan Fusheng, Cheng Renju et al. *Materials Science and Engineering A*[J], 2008, 489: 413
- Zhang Yan, Liang Wei, Wang Hongxia et al. *Rare Metal Materials and Engineering*[J], 2008, 37(11): 2023 (in Chinese)
- He Meifeng, Liu Lei, Wu Yating. *Corrosion Science*[J], 2008, 50: 3267
- Byeond Ho Kim, Kyung Chul Park, Yong Ho Park et al. *Materials Science and Engineering A*[J], 2011, 528: 808
- Song G L, Atrens A. *Advanced Engineering Materials*[J], 1999, 1: 11
- Bai Lijing, Zhang Hua, Yuan Ying et al. *Journal of Xi'an*

University of Technology[J], 2011, 27: 31 (in Chinese)

of Metals[J], 2007, 5: 18 (in Chinese)

23 Liu Fencheng, Liang Wei, Zhao Xingguo et al. Heat Treatment

表面纳米化对 AZ91D 镁合金渗铝行为的影响

张聪惠^{1,2}, 宋国栋¹, 王 婧¹, 赵 旭¹

(1. 西安建筑科技大学, 陕西 西安 710055)

(2. 陕西省冶金工程技术研究中心, 陕西 西安 710055)

摘 要: 镁合金表面渗铝是提高耐蚀性的一种有效方法。本研究将表面纳米化作为渗铝的预处理过程。采用高能喷丸对 AZ91D 镁合金进行表面纳米化处理, 然后进行真空铝扩散得到渗铝层。用透射电镜 (TEM) 和扫描电镜 (SEM) 观察了渗铝层的形貌。结果表明, 在对 AZ91D 镁合金表面高能喷丸后获得了 100 nm 的晶粒尺寸。在高能喷丸之后, 渗铝层的深度比未高能喷丸的渗铝层厚。在 440 °C 下扩散 12 h 后, 渗铝层的深度增加到 70 μm。采用电化学方法对 AZ91D 镁合金的耐腐蚀性能进行了表征。结果表明, 渗铝层明显降低了 AZ91D 镁合金的腐蚀速率。因此, 高能喷丸强化有利于镁合金表面渗铝, 提高镁合金的耐蚀性。

关键词: 高能喷丸; 表面纳米化; 铝扩散; 耐腐蚀性

作者简介: 张聪惠, 女, 1974 年生, 博士, 教授, 西安建筑科技大学冶金工程学院, 陕西 西安 710055, 电话: 029-82202547, E-mail: jiandazhang2010@hotmail.com